THE JOURNAL OF THE ACOUSTICAL SOCIETY OF KOREA VOL.23, NO.1E 2004. 3 pp. 24~30

A Study on Tunneling Effect in Sound Transmission Loss Measurement

Bong-Ki Kim*, Jae-Seung Kim**, Hyun-Sil Kim**, Hyun-Ju Kang**, Sang-Ryul Kim**
*Samsung Advanced Institute of Technology (SAIT), **Korea Institute of Machinery Materials
(Received February 17 2004; accepted March 18 2004)

Abstract

This study is aimed to evaluate a tunneling effect in the laboratory measurement of sound transmission loss. Based on the formulation for sound transmission loss of a finite panel in the presence of tunnel, variations of the sound transmission loss with the parameters of panel location and tunnel depth are investigated. In comparison with the transmission loss of a finite plate in an infinite rigid baffle, the maximum difference occurs in the laboratory measurement when the panel is placed at the center of the tunnel, while a better estimation of true transmission loss is obtained when the panel is located at either end

Keywords: *Sound transmission loss, Tunneling effect*

Ⅰ. Introduction

The sound insulation performance of a panel can be generally characterized by means of measurements of sound transmission loss (STL) in two reverberation chambers having a common aperture. A considerable effort has been devoted to match theoretical predictions with experimental measurements in reverberation chambers to establish the valid theoretical model[1,2]. From the standpoint of experimental method, reproducibility[3] in relation to consistency and accuracy of sound insulation measurements has been an important issue.

The majority of studies on reproducibility have been devoted to experimental investigations involving round robin tests.[3,4] The results indicate that different STLs from different laboratories were obtained even though the same panels were used for comparison. Such large discrepancies in reproducibility have seriously deteriorated the reliability of STL measurements, thus making it difficult to establish a valid analytical model for sound insulation.

Among the various reasons for the large deviations in reproducibility tests, an evident factor by experimentally proven is the so-called "tunneling effect"[5,6]. It is well-known that when measuring STL in a laboratory, the location of the specimen in an aperture obviously affects the results due to the tunneling effect. To better understand the tunneling effect, it will be necessary to develop a theoretical model for calculating the STL of a finite panel with the tunnel as shown in Figure. 1.

This paper deals with a two-dimensional system and is concerned with the STL of a finite panel, installed in a tunnel between the source and receiving room. A finite glass panel is considered as an example and the effects of tunnel depth, panel location are illustrated and the STL values are compared for the cases with and without tunnels.

Corresponding author: Bong-ki Kim (bkkim@kimm.re.kr)
Computational Science & Engineering Lab, Samsung Advanced Institute of Technology (SAIT), Giheung-eup, Yongin-si, Gyeonggi-do, 449-712, Korea

Ⅱ. Formulation

2.1. Representation of Acoustic and Vibration Fields

Figure 2 illustrates the two-dimensional acoustic fields arising from an incident plane wave with angle Δ. A single thin panel of finite height, h, and infinite width is placed in a rigid tunnel with a simply supported edge condition. Here, the harmonic term, $\exp(-i\omega t)$, will be omitted for convenience throughout. In region (I) depicted in Figure. 2, the total acoustic field then consists of the incident wave p_I^i, reflected wave p_I^r when the aperture is completely closed, and scattered wave p_I^s generated by the field in the aperture, which are respectively written as

$$p_I^i(x,y) = e^{ik\cos\theta(x+l_1)+ik\sin\theta\, y}, \tag{1}$$

$$p_I^r(x,y) = e^{-ik\cos\theta(x+l_1)+ik\sin\theta\, y}, \tag{2}$$

$$p_I^s(x,y) = \frac{1}{2\pi}\int_{-\infty}^{\infty} \beta_I^s(\zeta) e^{i\zeta y - ik_{x\zeta}(x+l_1)}\, d\zeta\ , \tag{3}$$

where $k_{x\zeta} = \sqrt{k^2-\zeta^2}$ and k is the wave number. Note that $p_I^s(-l_1, y)$ and $\beta_I^s(\zeta)$ are the Fourier-transform pair with the following relationships:

$$p_I^s(-l_1,y) = \frac{1}{2\pi}\int_{-\infty}^{\infty} \beta_I^s(\zeta) e^{i\zeta y}\, d\zeta \tag{4a}$$

$$\beta_I^s(\zeta) = \int_{-\infty}^{\infty} p_I^s(-l_1,y) e^{-i\zeta y}\, dy\ . \tag{4b}$$

In region (II) and (III), the total acoustic field can be represented by a summation of normal modes:

$$p_{II}(x,y) = \sum_{n=0}^{\infty}\left(A_n e^{ik_{xn}x} + B_n e^{-ik_{xn}x}\right)\cos(a_n y),$$
$$when\ -l_1 \le x \le 0\ and\ 0 \le y \le h\ , \tag{5}$$

$$p_{III}(x,y) = \sum_{n=0}^{\infty}\left(C_n e^{ik_{xn}x} + D_n e^{-ik_{xn}x}\right)\cos(a_n y),$$
$$when\ \ 0 \le x \le l_2\ and\ 0 \le y \le h\ . \tag{6}$$

Here, $k_{xn} = \sqrt{k^2 - a_n^2}$ and $a_n = \frac{n\pi}{h}$. In region (IV), the acoustic field can be expressed as the transmitted field:

$$p_{IV}^t(x,y) = \frac{1}{2\pi}\int_{-\infty}^{\infty} \beta_{IV}^t(\zeta) e^{i\zeta y + ik_{x\zeta}(x-l_2)}\, d\zeta\ . \tag{7}$$

Here, $p_{IV}^t(l_2, y)$ and $\beta_{IV}^t(\zeta)$ are the Fourier-transform pair which have the same relations as in Eqs.(4a,b).

The corresponding transverse displacement, $u(y)$, of a homogeneous thin plate to which the sound pressures of region (II) and (III) are applied is governed by

$$D\frac{\partial^4 u(y)}{\partial y^4} - \rho_s\omega^2 u(y) = \sum_{n=0}^{\infty}\left(A_n + B_n - C_n - D_n\right)\cos(a_n y), \tag{8}$$

where $D = E(1-i\eta)\frac{t^3}{12(1-\nu^2)}$, which is the bending stiffness. Here, ρ_s, E, η, t, and ν refer to the surface density, Young's modulus, loss factor, thickness, and Poisson's ratio of the plate, respectively. Assuming the boundary condition as simply supported, the plate displacement can be expressed as

$$u(y) = \sum_{m=1}^{\infty} E_m \sin(a_m y)\ , \tag{9}$$

where $a_m = \frac{m\pi}{h}$ and E_m is the amplitude of the m-th mode. Substituting Eq.(9) into Eq.(8), one obtains

$$\rho_s\sum_{m=1}^{\infty}\left(\omega_m^2 - \omega^2\right)E_m \sin(a_m y) = \sum_{n=0}^{\infty}\left(A_n + B_n - C_n - D_n\right)\cos(a_n y), \tag{10}$$

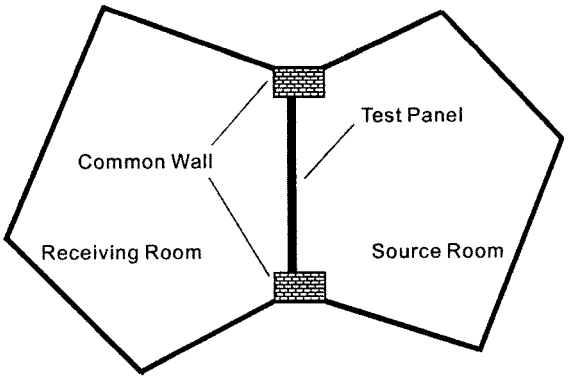

Fig. 1. Schematic illustration of the test facility for sound insulation measurement.

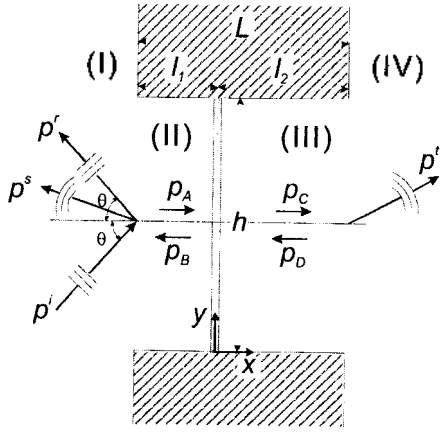

Fig. 2. Geometrical model for calculating sound transmission loss and acoustic field generated by plane wave incidence with angle.

where $\omega_m = \sqrt{\frac{D}{\rho_S}} a_m^2$ and means the *in-vacuo* natural frequency of the m-th mode.

2.2. Matching Boundary Conditions

From the boundary conditions of pressure continuity at the Interface at $x=-l_1$ along $0<y<h$, one can obtain

$$2e^{ik\sin\theta y} + \frac{1}{2\pi}\int_{-\infty}^{\infty} \beta_1^S(\zeta) e^{i\zeta y} d\zeta = \sum_{n=0}^{\infty}\left(A_n e^{-ik_{xn}l_1} + B_n e^{ik_{xn}l_1}\right)\cos(a_n y). \tag{11}$$

Normal velocity continuity gives

$$\frac{1}{2\pi}\int_{-\infty}^{\infty}(-ik_{x\zeta})\beta_1^S(\zeta) e^{i\zeta y} d\zeta = \sum_{n=0}^{\infty} ik_{xn}\left(A_n e^{-ik_{xn}l_1} - B_n e^{ik_{xn}l_1}\right)\cos a_n y. \tag{12}$$

In a similar fashion, the pressure and velocity continuities at $x=l_2$ along $0<y<h$ yield

$$\sum_{n=0}^{\infty}\left(C_n e^{ik_{xn}l_2} + D_n e^{-ik_{xn}l_2}\right)\cos(a_n y) = \frac{1}{2\pi}\int_{-\infty}^{\infty}\beta_{IV}^I(\zeta) e^{i\zeta y} d\zeta, \tag{13}$$

$$\sum_{n=0}^{\infty} ik_{xn}\left(C_n e^{ik_{xn}l_2} - D_n e^{-ik_{xn}l_2}\right)\cos(a_n y) = \frac{1}{2\pi}\int_{-\infty}^{\infty}(ik_{x\zeta})\beta_{IV}^I(\zeta) e^{i\zeta y} d\zeta \quad , \tag{14}$$

The plate displacement is coupled to the acoustic pressures

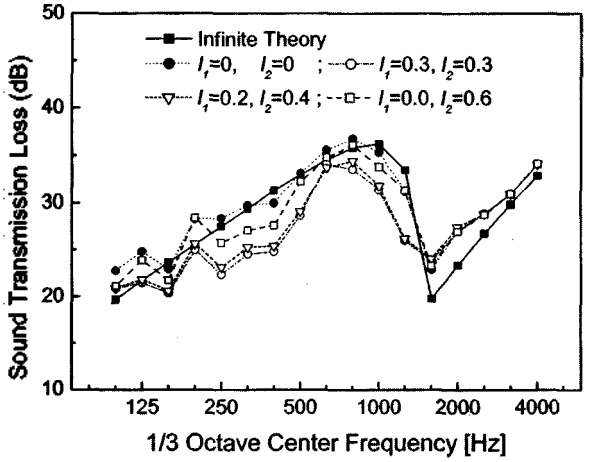

Fig. 3. Transmission loss for a glass panel of 2.4m-height between the cases without tunnel and with tunnel.

of the tunnel, thus the boundary conditions of both sides of the plate give

$$\sum_{m=0}^{\infty} ik_{xm}\left(A_m - B_m\right)\cos(a_m y) = \rho\omega^2\sum_{r=1}^{\infty} E_r \sin(a_r y), \tag{15}$$

$$\sum_{m=0}^{\infty} ik_{xm}\left(C_m - D_m\right)\cos(a_m y) = \rho\omega^2\sum_{r=1}^{\infty} E_r \sin(a_r y), \tag{16}$$

where ρ is the density of the air.

2.3. Solution of the Coupling Problem

Multiplying Eq.(10) by $\sin(a_r y)$ and integrating the both sides with respect to y from 0 to h, one then obtains

$$\rho_S\left(\omega_r^2 - \omega^2\right)E_r = \sum_{n=0}^{\infty}\left(P_n^{0^-} - P_n^{0^+}\right)Y_{nr} \quad . \tag{17a}$$

Here,

$$P_n^{0^-} = A_n + B_n, \; P_n^{0^+} = C_n + D_n, \tag{17b}$$

and

$$Y_{nr} = \frac{1-(-1)^{r+n}}{2(r+n)\pi} + \frac{1-(-1)^{r-n}}{2(r-n)\pi}. \tag{17c}$$

Once the numbers of vibration and acoustic modes are taken to be M and N, respectively, the surface pressures on both sides of the plate can be derived as the following matrix form:

$$\mathbf{P}^{0^-} = \mathbf{H}^{-1}\mathbf{QRE} - \mathbf{H}^{-1}\mathbf{X}, \tag{18}$$

$$\mathbf{P}^{0^+} = \mathbf{S}^{-1}\mathbf{TRE} \quad . \tag{19}$$

In the above expressions, $\mathbf{P}^{0^-}$ and $\mathbf{P}^{0^+}$ are both N-dimensional row vectors and H, Q, S, and T are $N \times N$ matrices whose elements are defined as

$$H_{mn} = \frac{ik_{xn}J_{mn}}{2\pi}\sin(k_{xn}l_1) - \varepsilon_m h\cos(k_{xm}l_1)\delta_{mn} \quad , \tag{20}$$

$$Q_{mn} = \frac{k_{xn}J_{mn}}{2\pi}\cos(k_{xn}l_1) - \varepsilon_m hi\sin(k_{xm}l_1)\delta_{mn}, \tag{21}$$

$$S_{mn} = \frac{ik_{xn}J_{mn}}{2\pi}\sin(k_{xn}l_2) - \varepsilon_m h\cos(k_{xm}l_2)\delta_{mn} \quad , \tag{22}$$

$$T_{mn} = -\frac{k_{xn} J_{mn}}{2\pi}\cos(k_{xn} l_2) + \varepsilon_m h i \sin(k_{xm} l_2)\delta_{mn},$$

$$k_{xn}, k_{xn} = \sqrt{k^2 - a_{m,n}^2}, \tag{23}$$

$$J_{m,n} = \int_{-\infty}^{\infty} \frac{\zeta^2\left[1-(-1)^m e^{i\zeta h}\right]\left[1-(-1)^n e^{-i\zeta h}\right]}{\left(\zeta^2 - a_m^2\right)\left(\zeta^2 - a_n^2\right)} d\zeta,$$

$m, n = 0, \ldots\ldots, N,$ (24)

and E is M-dimensional row vector having vibration mode coefficient, R, X are $N \times M$ matrix, $N \times 1$ row vector, respectively, the elements of which can be defined by

$$R_{nr} = \frac{\rho\omega^2}{ik_{xr}\varepsilon_r} Y_{nr}, \tag{25}$$

$$X_n = \frac{2ik\sin\theta\left[1-(-1)^n e^{ik\sin\theta h}\right]}{k^2\sin^2\theta - a_n^2}, \tag{26}$$

where $n = 0, \ldots\ldots, N$ and $r = 1, \ldots\ldots, M$.

Replacing Eqs.(18) and (19) into Eq.(17) allows the modal vector of plate displacement to be expressed in matrix form as

$$\mathbf{UE} = \mathbf{Y}(\mathbf{H}^{-1}\mathbf{Q} - \mathbf{S}^{-1}\mathbf{T})\mathbf{RE} - \mathbf{YH}^{-1}\mathbf{X}, \tag{27}$$

where U is $M \times M$ diagonal matrix with the r-th element as $\rho_s\left(\omega_r^2 - \omega^2\right)$. One can then obtain

$$\mathbf{E} = (\mathbf{YH}^{-1}\mathbf{QR} - \mathbf{YS}^{-1}\mathbf{TR} - \mathbf{U})^{-1}\,\mathbf{YH}^{-1}\mathbf{X}. \tag{28}$$

It is then possible to calculate the transmitted acoustic field from Eq.(19). The computation of Eq.(28) requires the calculation of the integral shown in Eq.(24). Unfortunately, a direct integration can not be used, since the integrand possesses singularities on the real axis. Accordingly, because the J_{mn} has four poles and two branch points in the

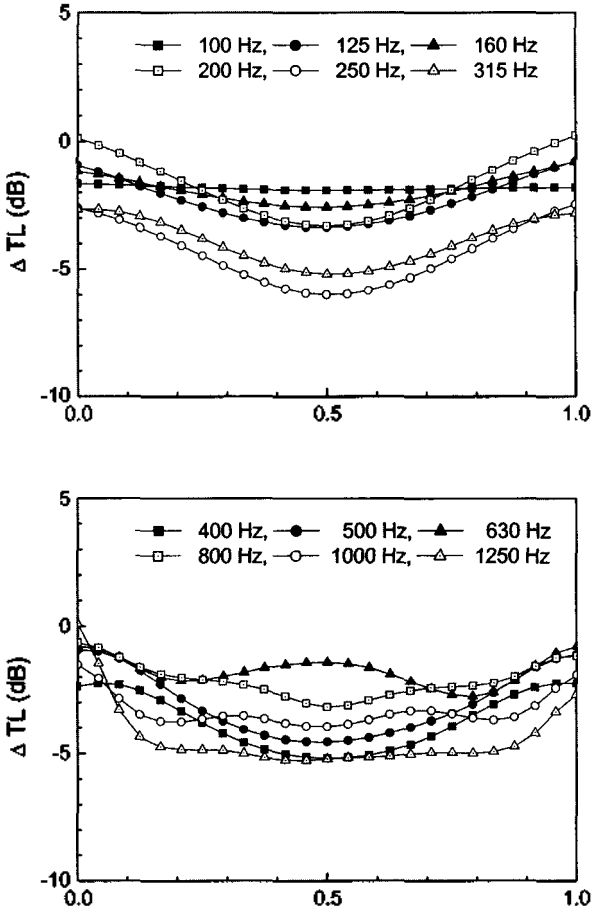

Fig. 4. Transmission loss change along the position of a glass panel of 2.4m-height in the tunnel of 0.6 m-depth.

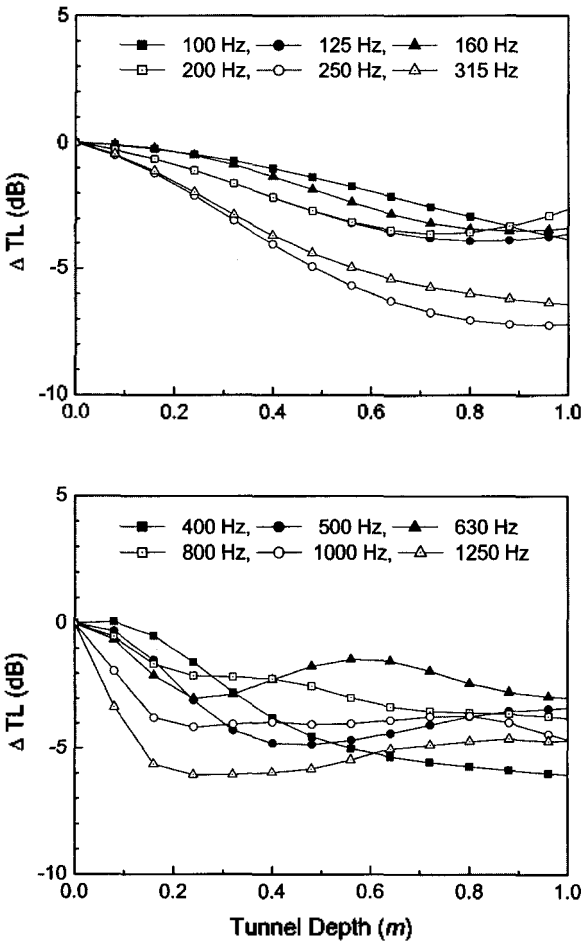

Fig. 5. Transmission loss change of a glass panel of 2.4m-height as increasing the tunnel depth where the panel is located at the center of tunnel.

complex ζ -plane an analytic contour integration is performed and gives

$$J_{mn} = \frac{2\pi h}{\sqrt{k^2 - a_m^2}} \varepsilon_m \delta_{mn} - 8i \int_0^{\infty} \frac{(1+iv^2)^2}{k^2 \sqrt{v^2 - 2i}\left[(1+iv^2)^2 - \beta_m^2\right]} \frac{\left[1-(-1)^r e^{ikh} e^{-kv^2 h}\right]}{\left[(1+iv^2)^2 - \beta_n^2\right]} dv, \quad (29)$$

where $\beta_{m,n} = a_{m,n} / k$. The second term of Eq.(29) denotes the cross modal coupling due to the end reflection at the interface. As the frequency increases, it can be negligible compared to the first term of Eq.(29) which corresponds to the propagating modes radiating the acoustic power into region (IV) on the condition of $k^2 > a_m^2$.

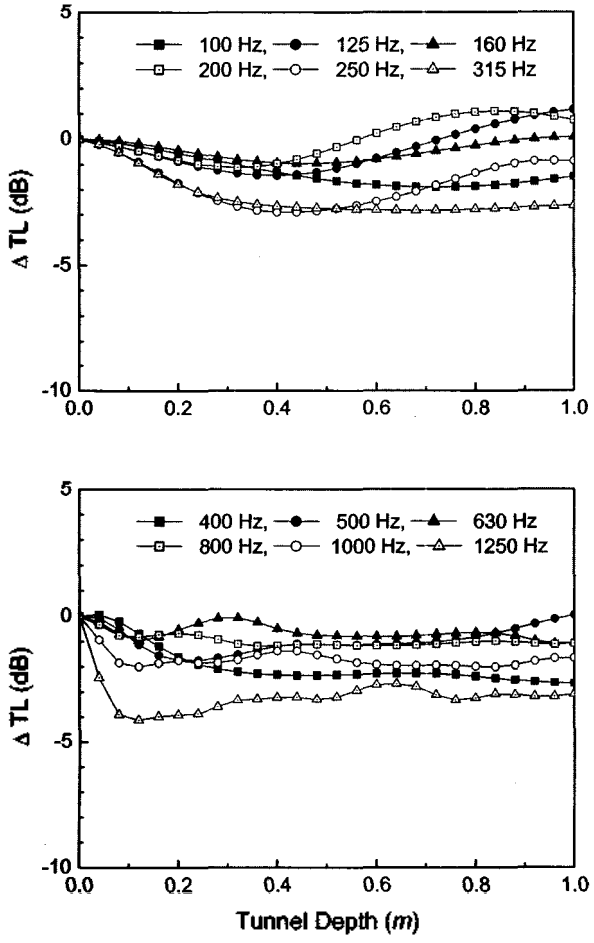

Fig. 6. Transmission loss change of a glass panel of 2.4m-height as increasing the tunnel depth where the panel is flush with the left-end of tunnel.

2.4. Sound Transmission Loss

The final step in the analysis is to find the transmission coefficient that can be expressed as the ratio of the transmitted acoustic power to the incident acoustic power. The incident acoustic power has the form of

$$\Pi_i = \frac{h}{2\rho c} \cos\theta, \quad (30)$$

and the transmitted acoustic power is as follows:

$$\Pi_t = \frac{1}{2} \mathrm{Re}\left[\int_0^h p(l_2, y)\, v^*(l_2, y)\, dy\right] = \frac{h}{2\rho\omega} \mathrm{Re}\left[\sum_{n=0}^{L} \varepsilon_n k_{xn}^* (C_n + D_n)(C_n - D_n)^*\right]. \quad (31)$$

Here, $Re[\ ]$ denotes the real part of [ ] and a symbol * indicates the complex conjugate. The modal coefficient C_n, D_n can be obtained from Eqs.(A13) and (A14). Since the power transmission coefficient can be given by $\tau(\theta) = \Pi_t / \Pi_i$, the random incidence STL can be expressed as

$$TL = 10 \log_{10}(1/\tau), \quad (32a)$$

where $\tau = \int_0^{\theta_{\lim}} \tau(\theta) \cos\theta\, d\theta \Big/ \int_0^{\theta_{\lim}} \cos\theta\, d\theta$. (32b)

Here, $\theta_{\lim}$ is the limit angle and taken as 78° throughout in the following analysis, which is based on field and laboratory measurements.[6]

III. Numerical Simulations

In this section, the result derived earlier is applied to a glass plate with a thickness of 9.2 mm. The material properties used in the following calculation are the same as those used by Sewell[7], i.e., ρt =23 kg/m^2, η=0.002, and ν=0.23. To validate the formulation in section I, the STL of the glass panel in the absence of a tunnel is compared to the infinite theory as shown in Fig. 3. The results in Fig. 3 indicate a reasonable agreement between infinite theory and the case without the tunnel, i.e. $(l_1, l_2) = (0, 0)$, differing by less than 2dB below the coincidence frequency.

3.1. Tunneling Effect

In the example presented in this section, a glass plate with a height of 2.4m is considered throughout. Three locations of the panel were selected by varying l_1 and l_2 as defined in Fig. 1: The center position of $(l_1, l_2) = (0.3, 0.3)\,m$, the flush position of $(l_1, l_2) = (0, 0.6)\,m$, and the proportional position of $(l_1, l_2) = (0.2, 0.4)\,m$ which is based on the ISO 140-3 recommendation.[3] By maintaining the depth of the tunnel and the height of panel as 0.6 m and 2.4 m, respectively, the STL of the plate corresponding to each location is calculated and the results are compared as depicted in Fig. 3. Below the coincidence frequency, a lower STL is obtained in all cases where the tunnel exists compared to the case without the tunnel. This is mainly due to the fact that the tunnel is capable of increasing resonance transmission. Note, however, that the STL is not affected by the existence of tunnel above the coincidence. It is also noteworthy that the center-position gives the lowest STL in comparison with the others. This is due to the fact that when the geometric shapes of both tunnels are identical, the acoustic mode of each tunnel readily interacts with each other through the panel, permitting the sound power to be efficiently transmitted. This explanation is generally consistent with previous results reported by Nilsson[8] and Schultz.[9]

3.2. Effect of Panel Location and Depth

For the simulation, the 1/3 octave band analysis is restricted to the frequency region below 1250 Hz because the tunnel significantly alters the STL in the frequency range below coincidence. Tunnel depths of 0.6m is used here for comparison and the changes in STL are shown as a function of normalized panel location, l_1/L. Figure 4 shows the STL difference, i.e., ΔTL, between the panels without a tunnel and with a 0.6 m-depth tunnel while moving the panel from source to receiver sides. Note that the results are symmetrical with respect to the center of the tunnel. As expected, the effect of the tunnel can be minimized for the case where the panel is flush with either end of the tunnel. Additionally, by placing the panel near the center position of the tunnel, the STL is found to be remarkably decreased in the frequency range below the coincidence.

The influence of tunnel depth on the tunneling effect is investigated in detail by increasing the depth from 0 to 1m. Figure 5 shows ΔTL of the center-located panel. The STL difference generally increases with increasing tunnel depth, especially in low frequency range. When the specimen is located at either end of the tunnel, the tunneling effect is greatly reduced compared to those of the center-located panel, although ΔTL gradually increases with tunnel depth as shown in Fig. 6. Hence, mounting a panel flush with the end of the tunnel can possibly improve the reproducibility of the STL obtained from different laboratories equipped with different tunnel depths.

IV. Conclusions

A theoretical analysis has been made on how a tunnel affects the STL. The presence of a tunnel can exert a significant influence on the STL measurements owing to its effect on panel vibration and radiation efficiency. Basically, the tendency is to increase the vibration and radiation efficiency of the plate which, in turn, reduce the transmission loss. It is interesting to note that, for the purpose of increasing the transmission loss, locating the panel flush with either end of the tunnel is preferred and this is closer to the analytical solution of a finite plate with the rigid baffle. As may therefore be expected, a definite increase in the STL with increasing the tunnel depth and decreasing the panel size was found. Consequently, the results confirm that the tunneling effect plays an important role in STL measurements and illustrate the possibility that the tunneling effect can be reduced, thus enhancing the reproducibility of STL measurements.

References

1. J. R. Callister, A. R. George, G. E. Freeman, "An empirical scheme to predict the sound transmission loss of single-thickness panels," J. Sound Vib, **222**, 145-151, 1999.
2. H. -J. Kang, J. -G. Ih, J. S. Kim, and H. S. Kim, "Prediction of sound transmission loss through multilayered panels by using Gaussian distribution of directional incident energy," J. Acoust. Soc. Am. **107**, 1413-1420, 2000.
3. ISO 140-2:1991 "Acoustics-Measurement of sound insulation in buildings and building elements-Part 2: Determination, verification and application of precision data" .
4. B. Rasmussen, "Repeatability and reproducibility of sound insulation measurements," Danish Acoustical Institute Technical report 118, 1984.

5. T. Kihlman and A. C. Nilsson, "The effects of some laboratory designs and mounting conditions on reduction index measurements," J. Sound Vib. 24, 349-364, 1972.
6. R. E. Jones, "Inter-comparisons of laboratory determinations of airborne sound transmission loss," J. Acoust. Soc. Am. 66, 148-164, 1979.
7. E. C. Sewell, "Transmission of reverberant sound through a single-leaf partition surrounded by an infinite rigid baffle," J. Sound Vib. 12, 21-32, 1970.
8. A. C. Nilsson, "Reduction index and boundary conditions for a wall between two rectangular rooms. Part I: Theoretical results," Acustica 26, 1-18, 1972.
9. T. J. Schultz, "Diffusion in reverberation rooms," J. Sound Vib. 16, 17-28, 1971.

[Profile]

● Bong-ki Kim

Bong-Ki Kim received B. S., M. S, and Ph. D degrees in 1990, 1992, and 1997, respectively, all from the department of Mechanical Engineering of KAIST. He was research engineer of NVH part at Samsung Motors technology center from 1997 to 1998. From 1999 to 2000, he joined the technical center of ArvinMeritor Exhaust in USA as a research engineer. Since 2000, he has been working with acoustics research group of KIMM. His research interests include sound field visualization, noise/vibration control.

● Jae-seung Kim

The Journal of the Acoustical Society of Korea, Vol.21, No.1E, 2002

● Hyun-sil Kim

The Journal of the Acoustical Society of Korea, Vol.21, No.1E, 2002

● Hyun-Ju Kang

The Journal of the Acoustical Society of Korea, Vol.21, No.1E, 2002

● Sang-Ryul Kim

The Journal of the Acoustical Society of Korea, Vol.21, No.1E, 2002